INVESTIGATING THE ENVIRONMENTAL IMPACT OF PYROLYSIS VOLATILES OF PRINTING PAPER UNDER A NITROGEN ATMOSPHERE

LE PAN,[*] JINXIANG CHEN,[*] CHUNFENG WAN,[*] HAO REN,[**]
HUAMIN ZHAI[**] and JINGJING ZHENG[***]

[*]*International Institute for Urban Systems Engineering & School of Civil Engineering, Southeast University, Nanjing, 210096, China*
[**]*Jiangsu Provincial Key Laboratory of Pulp and Paper Science and Technology, Nanjing Forestry University, Nanjing 210037, China*
[***]*School of Fashion, Zhejiang Sci-Tech University, Hang Zhou, 310018, China*
✉ *Corresponding author: Jinxiang Chen, chenjpaper@yahoo.co.jp*

Received November 26, 2013

The volatiles and environmental impact from the pyrolysis of printing paper at different temperatures were investigated using pyrolysis-gas chromatography/mass spectrometry (Py-G/MS) and scanning electron microscopy. There were 16 possible types of volatile matter present in the pyrolysis temperature range of 300 °C to 700 °C under a nitrogen atmosphere. A few of these volatiles were moderately toxic, but none was highly toxic or carcinogenic. The degree of carbonization with heat-induced inkless eco-printing (HIEP) was weaker than that with pyrolysis. Therefore, although HIEP produced small amounts of toxic substances, their quantities were low and could be controlled by optimizing the process conditions. Consequently, HIEP was found to be an ecologically and environmentally acceptable technology.

Keywords: eco-printing, printing paper, pyrolysis volatiles, environmental impact, G/MS

INTRODUCTION

Current laser and ink-jet printers produce harmful gases that pollute the environment, adding to regeneration costs and reducing paper quality.[1,2] In recent years, researchers in the printing industry have studied ecological inkless printing technology (also called inkless, zero-ink, or Zink technology). With the exception of inkless laser carbonized[3,4] printing technology, these technologies have thus far relied on particular features of the paper that is being printed. For example, ZINK Imaging Inc.[5] introduced a printing paper that contains a significant amount of crystalline dye. Based on a printing technique that causes various color changes in the paper due to exposure to heat during the printing process, ZINK developed the Pandigital inkless printer.[5] Dell Inc. created the Wasabi PZ310 mini-printer based on the principle that a special coating on photographic paper can reflect different wavelengths of light to produce a photo.[6] Other technologies rely on the nanostructural changes made to a special substance on the surface layer[7-9] or to a liquid polymer[10] during the printing process. The use of natural pigments[11-13] with ordinary printing paper represents a different type of eco-printing technology.[11-13] Inspired by the yellowing discoloration[14,15] of plant fibers, the authors recently proposed the radically new concept of heat-induced inkless eco-printing (HIEP),[16] which does not require ink during the printing process and which can achieve reliable printing results using an ordinary sheet of office paper. We have previously discussed a mechanism that results in negligible damage to the paper during HIEP.[17] Furthermore, HIEP has been proven not to suffer from either the severe carbonization of inkless laser printing or the significant ink consumption of current laser printing, which is considered to be the most ecologically friendly of the three printing technologies in existence.[18] However, HIEP may also produce a small amount of harmful gases, and the categorization, quantification, and environmental assessment of these volatiles require investigation and analysis to provide a scientific basis for designing safe HIEP technology. Because directly collecting volatiles during HIEP is difficult, this study consisted of an initial investigation of the volatiles produced and the environmental impact of HIEP by collecting volatiles using the paper pyrolysis method.

EXPERIMENTAL

Experimental material

Hoopoe® office paper (A4, 70 g/mm^2, white, from Dadong Pulp & Paper) was used in this study, and its composition has been described in the authors' previous paper.[16]

Experimental analysis of Py-GC/MS

The gas chromatography (GC) conditions were as follows: DB-5 column, helium (carrier gas), a column flux of 0.9 mL/min, a split ratio of 100:1, and the following column temperature increase progression. The initial temperature of 40 °C was maintained for 3 min and then ramped up to 300 °C at a rate of 15 °C/min and maintained for 5 min. The mass spectrometry (MS) conditions were as follows: electron impact (EI) ionization sources, temperature of 200 °C, electron energy of 70 eV, electron bombardment, full-scan mode, and a quality scan range (m/z) of 15-500. The samples were placed in a platinum boat, which was then dropped into the quartz pyrolysis tube in a free-fall manner. The pyrolysis volatiles were separated and identified using combined GC-MS (Shimadzu 2010). The total number of experimental samples was seven, and the pyrolysis temperature ranged from 300 °C to 700 °C (see Table 2) under a nitrogen (N2) atmosphere, with a pyrolysis time of approximately 0.1 s. The Mist spectral library search and normalization method were used to calculate the peak areas.

Microstructure observation

Following pyrolysis and simulated printing using HIEP and a currently available laser printer, the microstructures of the paper were observed using an Ultra Plus field emission scanning electron microscope (FE-SEM; Carl Zeiss NTS GmbH, Oberkochen, Germany).

RESULTS AND DISCUSSION

Categorization, quantity, and harmful effects of pyrolysis volatiles in printing paper

Figs. 1 (a, b) present the proton stream of the printing paper between 350 °C and 700 °C. Table 1 provides detailed data on the pyrolysis volatiles for a sample measured at 500 °C, including the volatilization time, area ratio, and formula. The mass spectra at the different temperatures shown in Figs. 1 (a, b) differ considerably from one another. For example, after the second minute, the crests between 300 °C and 700 °C (indicated by a Δ in Fig. 1) are mainly small and flat, but the crests from 350 °C to 500 °C (indicated by a ☆ in Fig. 1) are considerably sharper.

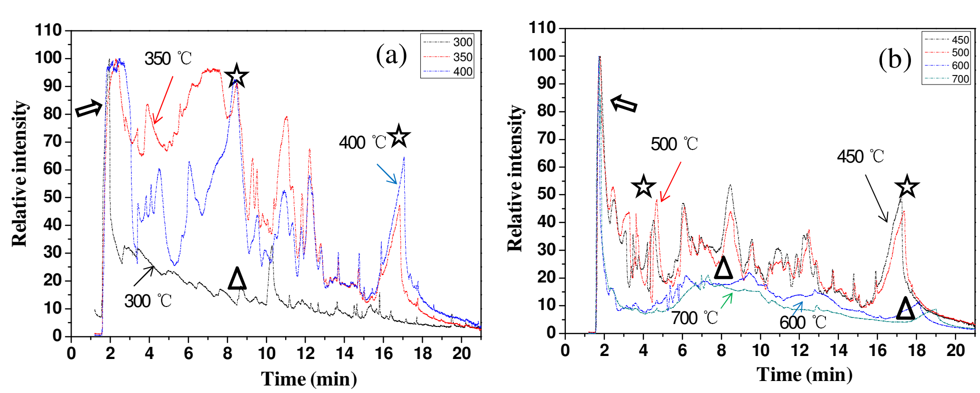

Figure 1: Proton stream of printing paper at different pyrolysis temperatures of (a) 350-450 °C and (b) 500-700 °C and (c) the substance (formula) of each pyrolysis volatile in detail

Table 1
The formula of each pyrolysis volatile in detail at 500 °C

No.	Line#	Time (min)	Area %	Formula	Mol. Weight
1	24	17.38	30.80	$C_6H_{10}O_5$	162
2	1	1.75	23.38	CO_2	44
3	13	8.47	10.54	$C_5H_6O_2$	128
4	7	4.69	8.40	$C_3H_6O_2$	74
5	9	6.11	5.22	$C_5H_6O_2$	98
6	3	3.26	4.71	$C_6H_{12}O_3$	132
7	18	12.49	3.42	$C_6H_{10}O_2$	114
8	2	2.45	2.29	$C_4H_6O_2$	86
9	6	4.37	2.28	$C_2H_4O_2$	60
10	5	3.63	1.99	CH_2O_2	46
11	14	9.59	1.79	$C_6H_8O_2$	112
12	17	11.94	0.79	$C_{11}H_{24}O$	172
13	16	11.42	0.72	$C_6H_{10}O_2$	114
14	20	13.72	0.51	$C_{10}H_{12}O_2$	164
15	21	14.83	0.49	$C_{10}H_{12}O_3$	180
16	15	10.54	0.47	$C_{10}H_{18}O_3$	186
17	8	5.78	0.43	$C_7H_{16}O_2$	132
18	19	12.85	0.40	$C_8H_{10}O_3$	154
19	10	6.53	0.36	C_5H_6O	82
20	23	15.95	0.26	$C_{11}H_{14}O_3$	194
21	4	3.56	0.25	$C_5H_8O_2$	100
22	12	6.99	0.18	$C_5H_8O_3$	98
23	11	6.87	0.17	C_8H_8	104
24	22	15.06	0.15	$C_{11}H_{14}O_3$	194

Accordingly, there are approximately 15 types of material at the low temperature of 300 °C and at the high temperatures of 600 °C or 700 °C, whereas there are approximately 25 types of material in the other cases. However, these proton stream photos taken at the second minute are similar in that they have particularly large peaks (Fig. 1, broad arrow) composed of CO_2 or H_2O.

Using the sample created at 500 °C as an example (Table 1), which contains many pyrolysis volatiles, we analyzed these volatiles and their contents. The area content of material No. 6 was less than 5%, whereas that of No. 7 was less than 4%. In fact, the total volatiles were minimal in the HIEP process; thus, this paper only analyzes the main volatiles with area contents of more than 4.5% (or 5%, when rounding up). Fig. 2 shows the main volatiles obtained at different temperatures and their formulas. The 16 types of volatiles were divided into six classes, as listed in Table 2, according to their toxicity (i.e., poisonousness or danger to the environment).[19-23] The toxicity properties of the class VI volatiles could not be identified, even after an extensive search of the literature. Class I includes non-toxic substances, whereas classes II and III contain irritants and flammable substances, respectively. The quantities of these volatiles obtained during the printing process were very small; thus, they could not cause fires or produce other major effects. Class IV includes corrosive substances, and there was only one type present at the temperature of 300 °C. Class V includes toxic substances that are moderately toxic. No highly toxic or carcinogenic substances were produced. Of the volatiles obtained after the pyrolysis of printing paper (see Table 2), those in non-toxic class I included No. 2 (CO_2) and No. 1 (H_2O), which were the main materials produced, whereas the mildly polluting classes II and III contained the greatest number of species, including No. 3 (C_4H_8O), No. 4 (C_4H_8O), No. 5 ($C_3H_6O_2$), No. 8 ($C_5H_6O_2$), No. 9 ($C_4H_8O_3$), No. 10 ($C_7H_{12}O$), No. 15 ($C_9H_{13}NO$), and No. 16 ($C_6H_{10}O_5$). As shown in Fig. 2, No. 16 ($C_6H_{10}O_5$) is levoglucosan,[24-26] which ranks third after water and carbon dioxide in terms of the total pyrolysis mass spectrometry area. This result indicates that the major pyrolysis product is levoglucosan, which is consistent with Wu's report[24] showing that the relative content of levoglucosan in the pyrolysis products of cellulose is 61% at 400 °C and 23% at 550 °C. The occurrence of volatiles in the more harmful classes, IV-V, was closely related to temperature. Two types of volatiles occurred within the temperature range of 300 °C to 400 °C, namely, No. 3 (C_4H_8O) and No. 7 ($C_5H_6O_2$), and two types of volatiles also occurred within the temperature range of 450 °C to 700 °C, namely, No. 5 ($C_3H_6O_2$) and No. 7 ($C_5H_6O_2$). There are many identical compounds among classes II-V that were found at the same temperature. To avoid repetitive statistics and to make the discovered issues more explicit, we placed each volatile in the highest class number (namely, the most harmful class) when it occurred in more than one of the classes (II-V). For example, substance No. 3 occurred in classes II-IV at a temperature of 300 °C, but we classified it in class IV and did not place it in the less harmful classes II and III (Fig. 3). Fig. 3 presents the area ratios of the substances produced at different temperatures after consolidating the repeated substances (if two or more substances existed, the area ratio was taken as the sum of the substances' area ratios). As shown in this figure, the type of the pyrolysis volatile material had a specific relationship with the pyrolysis temperature. The area contents of all volatiles at temperatures of 300 °C to 700 °C had similar characteristics at both extremes (i.e., the high and low temperatures) and had opposite characteristics at the intermediate temperatures.

Table 2
Toxicity classification of pyrolysis volatiles obtained at 300-700 °C

Temperature (°C)	300	350	400	450	500	600	700
I. Non-toxic	1	1	1	2	2	1,2	2
II. Irritant	3, 9	16	16	16	8, 16	10, 16	15, 16
III. Flammable	3	4		5	5, 8	5, 10	
IV. Corrosive	3						
V. Toxic			7	5, 7	5, 7	5	
VI. Unknown*		12	6, 14		13		11

*The toxicity properties could not be identified even after an extensive search of the literature.[19-23] The numbers correspond to those in Table 1

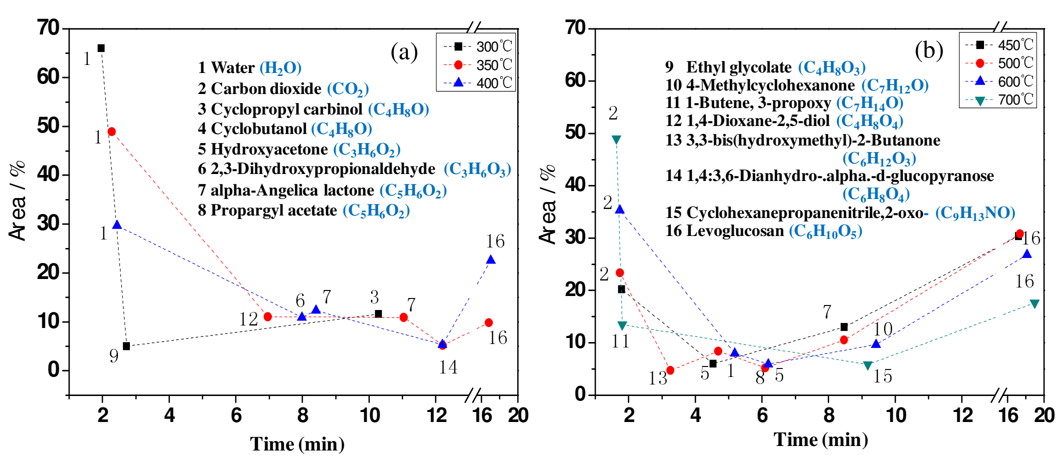

Figure 2: Substance (formula) for each pyrolysis volatile produced when printing paper at (a) 300-400 °C and (b) 450-700 °C

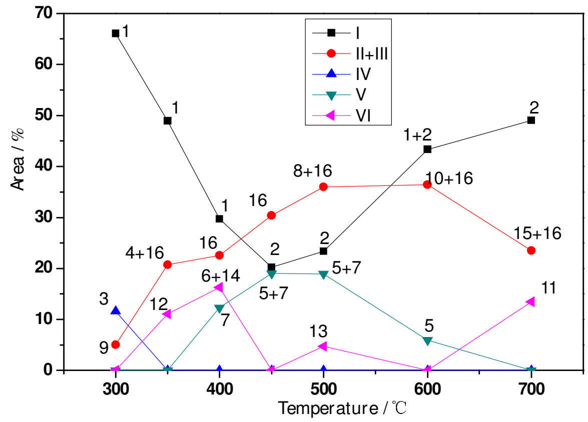

Figure 3: Area contents of the main products at different temperatures

The number of species present at each temperature was not excessive in either the mildly polluting classes II and III or the more harmful classes IV-VI. Based on the content (area ratio) of each substance, the non-toxic class I had the largest content: half of these substances had a content of approximately 50%, with the highest being 66% and the lowest being 20%. When the content of class I was lower, the content of the mildly polluting substances was higher between 400 °C and 600 °C. Overall, the total content of non-toxic class I and mildly polluting class II-III substances was greater than 70%. There was only one substance that belonged to the more harmful class IV at 300 °C (Fig. 3, indicated by ▲). The content of class V substances, which are moderately toxic, was 15-20% between 400 °C and 500 °C (indicated by ▲ in Fig. 3). This content is moderately low, but class V substances are not highly toxic or carcinogenic. Over the larger range of temperatures, the class VI content was less than 5% (Fig. 3, indicated by ▼), which will facilitate the selection of the optimal temperature for environmentally friendly printing.

Microstructure of HIEP printing paper and its environmental impact

The volatiles from the printing paper were related not only to the pyrolysis temperature, but also to the heating duration, which was closely related to the degree of the heating effect. Therefore, we combined these results with the degree of heating to draw a more accurate conclusion regarding the volatiles produced during heat printing according to the pyrolysis mass spectrometry results. As stated in the experimental conditions, the pyrolysis time was 0.1 s. However, during the mass spectrometry experiment, the sample remained at the bottom of the pyrolyzer (with an environmental temperature of approximately 280 °C) and was not directly removed until the end of the experiment (approximately 30 min), after the sample was dropped into a quartz pyrolysis tube. However, scan printing is a continuous process, and thus, the contact time of each point was approximately 0.03-0.09 s at 350-480 °C, according to the previous report. Thus, the heating time was shorter than the pyrolysis time, and the HIEP heating degree was weaker. We were temporarily unable to measure the contact time for click printing due to the manual nature of its operation. However, heat printing does release pyrolysis volatiles, so we are able to discuss the possible volatiles released and the environmental impact of HIEP based on the microstructure of the printing paper.

Microstructure of printing paper with different thermal effects

The microstructures of the printing paper following the currently available laser printing,[18] pyrolysis,[18] and laser inkless eco-printing (LIEP)[17] processes are shown in Fig. 4, Fig. 5, and Fig. 6, respectively. Fig. 4 presents the fibers (denoted by a broad arrow), voids (denoted by a "v"), and a small amount of particles (Fig. 4, denoted by a triangle) in a position not covered by toner. The fibers are composed of cellulose or hemicellulose[27-29] and are the major component of the paper. The mutual superposition of fibers leads to the formation of many recesses and voids.[30] The particles are inorganics[29,30] (filler or additive agents, typically sorted as "ash"), which are added during the papermaking process. Fig. 5 shows that there are thinner fibers (indicated by a broad arrow) and more particles (denoted by a triangle) after pyrolysis at the higher temperature.[31] A comparison of the differences in the paper's microstructure after pyrolysis (Figs. 5b, d) and LIEP (Fig. 6) reveals that the pyrolysis did not cause the clear carbonization phenomena, the number of small holes (Fig. 6, circle markers), and the cauliflower core-like clots (Fig. 6, triangle markers) that were caused by LIEP.

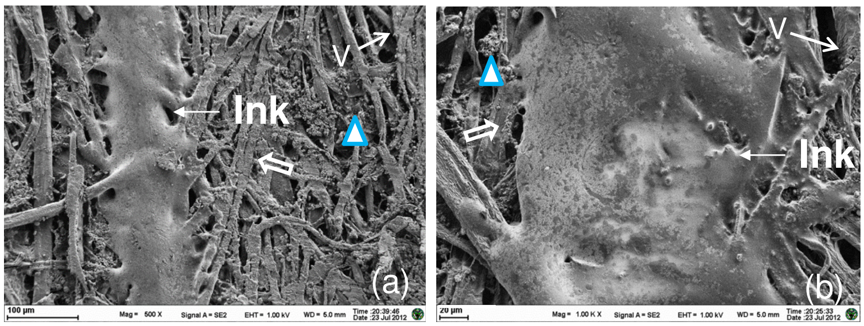

Figure 4: Microstructure of the paper surface after currently available laser printing: (a) low-magnification and (b) high-magnification images

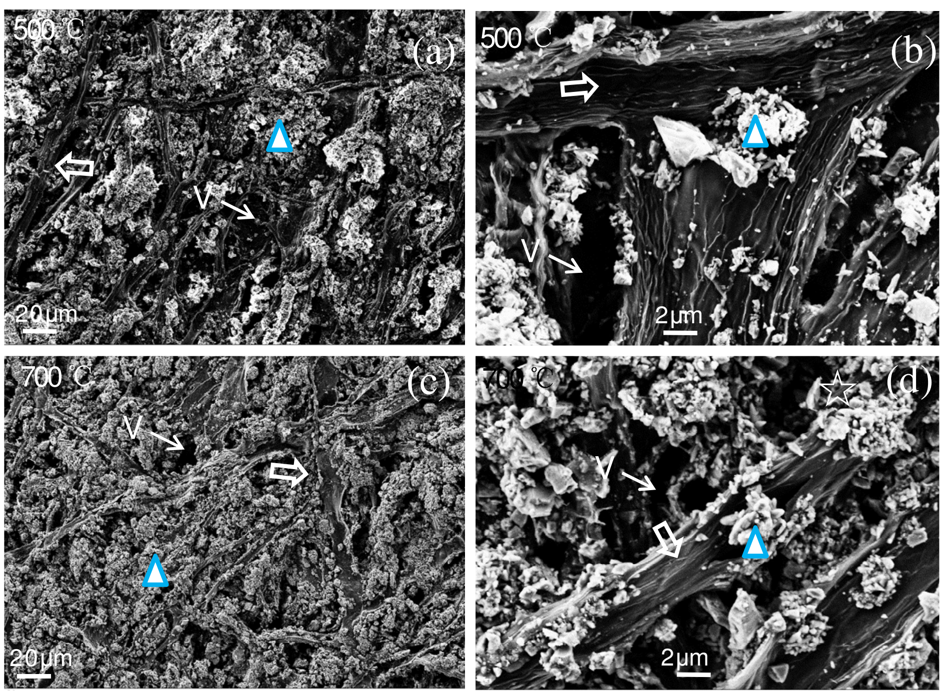

Figure 5: Microstructure of the printing paper after pyrolysis at different temperatures: (a, c) low-magnification and (b, d) high-magnification images

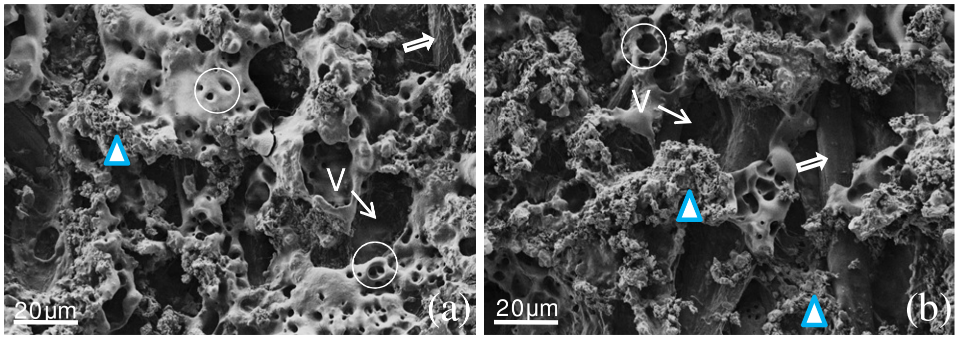

Figure 6: Microstructure of the printing paper in text areas after LIEP: (a) small holes (circle markers) and (b) cauliflower core-like clots (triangle markers); the broad arrow indicates a fiber and letter “v” indicates an irregular void

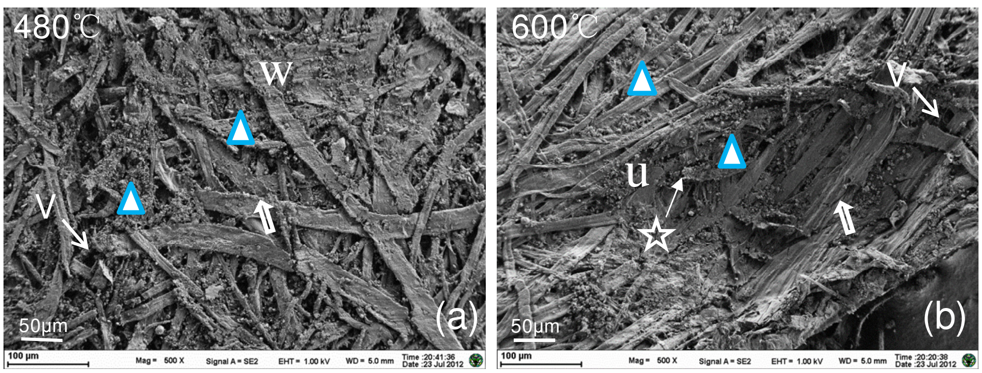

Figure 7: Paper surface microstructure at different temperatures with (a) scan printing and (b) click printing

Next, as shown in the microstructure image (Fig. 7a), slight scratches were left on the paper surface after scan printing (Fig. 7a, denoted by a "w"), but very obvious concave indentations were left after click printing (Fig. 7b, denoted by a "u").[18] The microstructures differed in appearance following treatment at different temperatures. The change was minimal for scan printing (Fig. 7a), and the microstructures were similar to those obtained without laser printing (Fig. 4, denoted by a broad arrow). However, the fibers on the surface of the concave indentations appeared flatter (Fig. 7b, denoted by a broad arrow) or even crushed (Fig. 7b, denoted by an asterisk) after click printing. Moreover, the ash particulate matter slightly increased (Fig. 7b, denoted by a square), but not in an obvious manner. Therefore, compared with the microstructure obtained with pyrolysis in which the fibers were dense, scattered, and identical, as with many flocculent particles (Fig. 5), obvious carbonation phenomena were not observed among the fibers after HIEP (Fig. 7, denoted by a broad arrow), excluding the concave indentations obtained after heat click printing. There were two reasons for this behavior: a) the pyrolysis time was longer than that of HIEP, and b) the sample remained at the bottom of the pyrolyzer at a temperature of approximately 280 °C for up to 30 min. Therefore, the degree of heating from the HIEP process was lower than that of pyrolysis, and thus, the sample subjected to HIEP did not exhibit clearer carbonization from a visual standpoint than the residue after pyrolysis.

Environmental benefits of HIEP

As mentioned above, compared with the microstructure and degree of heating, pyrolysis clearly produced more residue than HIEP. Thus, HIEP released less volatile matter than pyrolysis. As shown in Table 2 and Fig. 3, the volatiles produced by the printing paper were analyzed next. The summed content of non-toxic class I and lightly polluting classes II-III substances was greater than 70%. The largest number of toxic class V substances whose area was 15-20% (indicated by ▼ in Fig. 3) was only two, in the temperature range of 400 °C to 500 °C. The content of these substances was moderately low, but they are only moderately toxic, not highly toxic or carcinogenic. There was generally only one substance from class V at each temperature over the larger range of temperatures.

Table 2 includes substances whose chemical properties were not determined (Class VI). Even if these substances are toxic, the content of most of them was less than 5%, so their effect would not be significant. The degree of heating during HIEP differed considerably from that of pyrolysis, indicating that HIEP produces toxic substances in small amounts and does not produce highly toxic or carcinogenic substances. Considering that the actual printing process requires a certain printing speed, future temperatures should be above 400 °C, preferably between 500 °C and 700 °C, a temperature range that only produced one class IV substance at most. Even if the volatiles released from this process were restricted to the most harmful types of molecules (Nos. 4 or 11), we could also change the temperature to avoid producing toxic and carcinogenic substances. The printing paper surface adsorbed a considerable amount of toner during laser printing (Fig. 4), whereas the surface subjected to the HIEP process acquired only some indentations and recesses, without producing many volatiles.

In summary, HIEP is an environmentally friendly process that does not consume toner or ink and that does not cause carbonization.[32-34] Thus, HIEP technology significantly reduces the waste paper recycling costs associated with ink processing, and its use provides excellent economic and environmental benefits.[18] The substances that form during the decomposition process must be identified, and their content, toxicity, and effect on the yellow discoloration observed during this process must be determined. Moreover, the analysis method used in this paper provides a reasonable approach for determining the environmental impact of HIEP.

CONCLUSION

By analyzing the volatiles released during pyrolysis using a nitrogen atmosphere and the microstructure and degree of heating of printing paper, this study primarily discussed the possible volatiles released and the protection of the surrounding environment associated with HIEP. The following conclusions were drawn:

(1) When the pyrolysis temperature was between 300 °C and 700 °C, the printing paper typically produced 16 types of volatiles. One or two toxic substances were present at each temperature, but these substances are not highly toxic or carcinogenic. The content of moderately toxic substances was less than 5%, which will facilitate the selection of the optimal temperature for environmentally friendly printing.

(2) The degree of carbonization with HIEP was weaker than that with pyrolysis, and thus, the quantity of volatiles after HIEP was lower than that after pyrolysis. Therefore, even though HIEP produced a small amount of toxic substances, their area content was less than that of the volatiles released during pyrolysis.

(3) We could optimize the process parameters to develop a more ecological and environmentally friendly printing technology. Furthermore, unlike laser printing, HIEP does not consume large quantities of toner. Thus, HIEP technology could significantly reduce paper recycling costs without increased ink processing, and its use is associated with economic and environmental benefits.

ACKNOWLEDGMENTS: This work was supported by the Peak of Six Personnel in Jiangsu Province (No. 2012-JNHB-013).

REFERENCES

[1] M. H. Chantignya, D. A. Angers and C. J. Beauchamp, *Soil Biol. Biochem.*, **32**, 1561 (2000).
[2] A. M. Faul, *Cellulose Chem. Technol.*, **44**, 451 (2010).
[3] N. M. Yao and X. L. Zhao, Printing paper carbonization method with laser high temperature. ZL 200710071837.5 (in Chinese).
[4] J. Chen, L. Xu, J. Xie, Y. Wang, Y. L. Pan *et al.*, *Cellulose Chem. Technol.*, (in press).
[5] X. M. Song and S. L. Wang, *Publishing and Printing*, **3**, 44 (2010) (in Chinese).
[6] http://en.community.dell.com/dell-blogs/direct2dell/b/direct2dell/archive/2009/02/10/inkless-wasabi-pz310-printer-weighs-7-ounces.aspx
[7] A. A. Shestopalov, R. L. Clark and E. J. Toone, *J. Am. Chem. Soc.*, **129**, 13818 (2007).
[8] S. J. Choi and J. Y. Park, *Small*, **6**, 371 (2010).
[9] A. A. Shestopalov, R. L. Clark and E. J. Toone,

Langmuir, **26**, 1449 (2010).
[10] H. N. Yow and A. F. Routh, *Soft Matter*, **2**, 940 (2006).
[11] T. Rentschler, *Wochenbl. Papierfabr.*, **133**, 1385 (2005).
[12] H. M. El-Hennawi, K. A. Ahmed and I. Abd El-Thalouth, *Indian J. Fibre Text.*, **37**, 245 (2012).
[13] I. Wataoka, *J. Soc. Fiber Sci. Technol.*, **68**, 176 (2012) (in Japanese).
[14] M. Beyer, H. Koch and K. Fischer, *Macromol. Symp.*, **232**, 98 (2005).
[15] D. Fromageot, N. Pichon, O. Peyron and J. Lemaire, *Polym. Degrad. Stabil.*, **91**, 347 (2006).
[16] J. Chen, Y. Wang, J. Xie, C. Meng, G. Wu *et al.*, *Carbohyd. Polym.*, **89**, 849 (2012).
[17] J. Xie, J. Chen, Y. Wang, Y. Liu, M. N. Noori *et al.*, *Cellulose Chem. Technol.*, **48**, 577 (2014).
[18] J. Chen, J. Xie, L. Pan, X. Wang, L. Xu *et al.*, *J. Wood Chem. Technol.*, **34**, 202 (2014).
[19] http://www.ichemistry.cn/ (January 10, 2014).
[20] http://www.chemicalbook.com/ProductIndex_ EN. aspx/ (January 10, 2014).
[21] http://toxnet.nlm.nih.gov/ (January 10, 2014).
[22] http://www.ncbi.nlm.nih.gov/pubmed/ (January 10, 2014).
[23] http://www.hmdb.ca/ (January 10, 2014).
[24] Y. M. Wu, Z. L. Zhao, H. B. Li, and F. He, *J. Fuel Chem. Technol.*, **37**, 427 (2009) (in Chinese).
[25] A. Aho, M. Käldström, P. Fardim, N. Kumar, K. Eränen *et al.*, *Cellulose Chem. Technol.*, **44**, 89 (2010).
[26] M. Ursescu, G. Lisa, C. Malutan, S. Ciovica, *Cellulose Chem. Technol.*, **43**, 427 (2009).
[27] N. Mosier, C. Wyman, B. Dale and R. Elander, *Bioresour. Technol.*, **96**, 673 (2005).
[28] G. P. Chen and C. R. Li, *China Pulp Pap. Ind.*, **31**, 79 (2010) (in Chinese).
[29] H. A. Carter, *J. Chem. Educ.*, **73**, 1068 (1996).
[30] M. Alava and K. Niskanen, *Rep. Prog. Phys.*, **69**, 669 (2006).
[31] C. Vasile, C. M. Popescu, M. C. Popescu, M. Brebu, S. Willfor, *Cellulose Chem. Technol.*, **45**, 29 (2011).
[32] E. Biagini, F. Barontini and L. Tognotti, *Ind. Eng. Chem. Res.*, **45**, 4486 (2006).
[33] K. Elyounssi, J. Blin and M. J. Halim, *Anal. Appl. Pyrol.*, **87**, 138 (2010).
[34] M. M. Tang and R. Bacon, *Carbon*, **2**, 211 (1964).